Ligand Binding to the Fe(III)-Protoporphyrin IX Complex of Phosphodiesterase from *Escherichia coli* (*Ec* DOS) Markedly Enhances Catalysis of Cyclic di-GMP: Roles of Met95, Arg97, and Phe113 of the Putative Heme Distal Side in Catalytic Regulation and Ligand Binding[†]

Atsunari Tanaka[‡] and Toru Shimizu*

Institute of Multidisciplinary Research for Advanced Materials, Tohoku University, Sendai 980-8577, Japan

Received June 27, 2008; Revised Manuscript Received October 21, 2008

ABSTRACT: Phosphodiesterase (*Ec* DOS) from *Escherichia coli* is a gas-sensor enzyme in which binding of gas molecules, such as O_2, CO, and NO, to the Fe(II)-protoporphyrin IX complex in the sensor domain stimulates phosphodiesterase activity toward cyclic-di-GMP. In this study, we report that external axial ligands, such as cyanide or imidazole, bind to Fe(III)-protoporphyrin IX in the sensor domain and induce a 10- to 11-fold increase (from 8.1 up to 86 min^{-1}) in catalysis, which is more substantial than that (6.3 to 7.2-fold) observed for other gas-stimulated Fe(II) heme-bound enzymes. Catalytic activity (50 min^{-1}) of the heme-free mutant, H77A, was comparable to that of the ligand-stimulated enzymes. Accordingly, we propose that the heme at the sensor domain inhibits catalysis and that ligand binding to the heme iron complex releases this catalytic suppression. Furthermore, mutations of Met95, Arg97, and Phe113 at the putative heme distal side suppressed the ligand effects on catalysis. The rate constants (19,000 $\times$ 10^{-5} $\mu M^{-1}min^{-1}$) for cyanide binding to the M95A and M95L mutants of the full-length enzyme were 633-fold higher than that to wild-type *Ec* DOS (30 $\times$ 10^{-5} $\mu M^{-1}min^{-1}$). The absorption spectrum of the F113Y mutant suggests that the Tyr O^- group directly coordinates to the Fe(III) complex and that the cyanide binding rate to the mutant is very slow, compared with those of the wild-type and other mutant proteins. We observed a similar trend in the binding behavior of imidazole to full-length mutant enzymes. Therefore, while Met95 and Phe113 are not direct axial ligands for the Fe(III) complex, catalytic, spectroscopic, and ligand binding evidence suggests that these residues are located in the vicinity of the heme.

Escherichia coli phosphodiesterase (*Ec* DOS[1]) is a gas-sensor enzyme that displays 6- to 7-fold enhanced catalytic activity toward cyclic diGMP (c-diGMP) upon the binding of O_2, CO, or NO gas to the Fe(II)-protoporphyrin IX complex (Fe(II) complex) in the sensor domain (*1*). The gas responsive characteristics of this enzyme are novel since all other gas-sensor proteins reported to date recognize and respond to selective gas molecules (*2*−*6*). O_2 and CO gas molecules bind only to the Fe(II) complex. *Ec* DOS appears to be an oxygen sensor enzyme since it is unlikely that CO or NO exist at concentrations higher than O_2 inside the cells.

The autoxidation rate (0.015 min^{-1}) of full-length *Ec* DOS (*7, 9*) is high, compared with that of AxPDEA1 (<0.001 min^{-1}) (*8*), another heme-bound oxygen sensor enzyme with the same substrate, c-diGMP, from *Acetobacter xylinum* (*9*). In addition, the full-length *Ec* DOS enzyme is mostly purified as the Fe(III) form in the absence of reductant from the *E. coli* overexpression system under our conditions (*1, 7, 8*). The redox potential (+70 mV vs SHE) of *Ec* DOS is significantly lower than those (+140−269 mV vs SHE) of cytochromes *c* and b_{562} but similar to that (+40−50 mV vs SHE) of myoglobin (*10, 11*). Therefore, it is important to determine the catalytic activities of Fe(III) complex-bound *Ec* DOS together with the catalytic changes caused by adding external ligands to the Fe(III) complex. Additionally, examination of catalysis by the heme-free enzyme is essential to elucidate the role of the heme iron in this process.

X-ray crystal analysis of the isolated Fe(III) complex-bound PAS domain discloses that the tertiary structure of the heme distal side (in particular, between residues 86 and 97) is considerably flexible and thus difficult to resolve. However, the crystal structures of Fe(II)-complex- and O_2-

[†] This work was supported in part by a Grant-in-Aid and by the Special Education and Research Expenses from the Ministry of Education, Culture, Sports, Science and Technology of Japan to T.S.

* To whom correspondence should be addressed. Institute of Multidisciplinary Research for Advanced Materials, Tohoku University, 2-1-1 Katahira, Aoba-ku, Sendai 980-8577, Japan. Tel:+81-22-217-5604, 5605. Fax: +81-22-217-5604, 5390. E-mail: shimizu@tagen.tohoku.ac.jp.

[‡] Present address: The Wistar Institute, Philadelphia, PA 19104.

[1] Abbreviations: *Ec* DOS, direct oxygen sensor from *Escherichia coli* or a phosphodiesterase from *Escherichia coli* with the substrate, cyclic-dinucleotide-GMP; c-diGMP, cyclic-dinucleotide-GMP; l-di-GMP, linear-dinucleotide-GMP; Fe(II) complex, Fe(II)-protoporphyrin IX complex; Fe(III) complex, hemin or Fe(III)-protoporphyrin IX complex; pET28a(+)-*Ec* DOS, the expression plasmid pET28a(+) with *Ec* DOS cDNA inserted; CBS, cystathionine β-synthase with a heme as a redox and/or CO sensor; CooA, a CO-sensing transcriptional factor from the photosynthetic bacterium *Rhodospirillum rubrum*; FixL, a heme-binding oxygen sensor kinase; sGC, soluble guanylate cyclase; AxPDEA1, a heme-regulated phosphodiesterase toward c-diGMP from *Acetobacter xylinum*.

10.1021/bi8012017 CCC: $40.75
Published on Web 11/18/2008

Fe(II) complex-bound PAS domain have been successfully determined (*12, 13*). These structures show that Met95 is the axial ligand for the Fe(II) complex and that Arg97 binds directly to the O_2 coordinated to the Fe(II) complex. Phe113 is located in the vicinity of the O_2 molecular bond to the Fe(II) complex and influences catalysis and ligand access behavior. While the structure of the heme distal side of Fe(III) complex-bound *Ec* DOS is unknown at present, it is important to determine the effects of the amino acids essential for catalysis by the Fe(II) complex-bound enzyme on the catalytic activity and ligand-binding kinetics of the full-length Fe(III) complex-bound *Ec* DOS enzyme.

In the present study, we show that the Fe(III) complex enzyme displays catalytic activity toward c-diGMP that is analogous to that of the Fe(II) complex *Ec* DOS. Interestingly, catalysis was markedly enhanced by adding the external ligands, cyanide, and imidazole, to Fe(III) hemin, similar to the results observed for the gas-stimulated Fe(II) complex-bound enzyme. Importantly, the heme-free enzyme displayed high catalytic activity comparable to that of the ligand-induced enzyme. To elucidate the underlying molecular mechanism of catalytic enhancement by ligands, we generated Fe(III) complex-bound full-length *Ec* DOS proteins mutated at Met95, Arg97, and Phe113 in the putative distal side, and examined their catalytic activities and spectral characteristics in the absence and presence of the external axial ligands, cyanide and imidazole. Our catalytic and spectrometric findings indicate that Met95 and Phe113 are located in sufficiently close proximity to the ligand access channel of the Fe(III) complex to influence catalytic enhancement caused by ligand binding, heme coordination structure, and ligand binding kinetics. We further discuss the molecular mechanism of intramolecular signal transduction of *Ec* DOS in association with the roles of the heme iron complex and heme distal amino acids in catalysis and ligand binding.

EXPERIMENTAL PROCEDURES

Materials. All chemical reagents were of the highest available grade. Reagents were purchased from Wako Chemicals (Osaka, Japan) and used without further purification. Calf intestine alkaline phosphatase (CIAP) was obtained from Takara Bio (Otsu, Japan), c-diGMP from BIOLOG (Bremen, Germany), 6-(2-hydroxy-1-methyl-2-nitrosohydrazine)-*N*-methyl-1-hexanamine (NOC9) from DOJINDO (Kumamoto, Japan), and BIOMOL GREEN reagent from Biomol (Plymouth Meeting, PA). The QuikChange site-directed mutagenesis kit from Stratagene (La Jolla, CA) was employed. Oligonucleotides for plasmid construction and site-directed mutagenesis were acquired from Nihon Gene Research Lab (Sendai, Japan).

Construction of the Expression Plasmid and Site-Directed Mutagenesis. Cloning of *Ec* DOS and construction of the expression plasmid, pET28a(+)-*Ec* DOS, were performed as described previously (*9*). Site-directed mutagenesis was performed with the QuikChange kit. The H77A, M95A, M95L, M95H, R97A, R97I, and R97E mutants were generated according to previous reports (*1, 9*). Phe113 mutants were generated using the following oligonucleotides (*1, 9*). F113A: forward, 5′ aaaatctggacccgtGCGgcgctatcgaaagtg 3′; reverse, 5′ cactttcgatagcgcCGCacgggtccagatttt 3′. F113T: forward, 5′ aaaatctggacccgtACCgcgctatcgaaagtg 3′; reverse, 5′ cactttcgatagcgcGGTacgggtccagatttt 3′. F113Y: forward, 5′ aaaatctggacccgtTATgcgctatcgaaagtg 3′; reverse, 5′ cactttcgatagcgcATAacgggtccagatttt 3′. The upper case letters indicate the mutated sequences. All mutations were confirmed by DNA sequencing.

Protein Expression and Purification. Wild-type and mutant *Ec* DOS proteins were overexpressed in the *E. coli* strain, BL21(DE3), and transformed with the pET28a(+)-*Ec* DOS expression plasmid containing an N-terminal His_6 tag and thrombin cleavage site. Culture conditions for *E. coli* and protein purification procedures were based on a previous report (*1*). Purified proteins were treated with 1 mM potassium ferricyanide for full oxidation. After dialysis against 20 mM Tris-HCl at pH 8.0, containing 5% glycerol, oxidized proteins were concentrated with an Amicon Centriprep (Millipore, Billerica, MA) and Centrisart I (Sartorius Stedim Biotech, Aubagne, France). Samples were stored at −20 °C in the presence of 40% glycerol.

Optical Absorption Spectroscopy. All static spectral data were obtained using a UV-2500PC (Shimadzu, Kyoto, Japan) spectrophotometer. To measure the rapid reactions of ligand association to heme, we used a stopped-flow mixing apparatus, RSP-1000 (Unisoku, Osaka, Japan). All measurements were performed at 25 °C using a temperature controller. The reaction buffer used was 50 mM Tris-HCl and 50 mM NaCl at pH 8.0.

Determination of the Kinetic Parameters of Cyanide and Imidazole Binding to Wild-Type and Mutant Ec DOS. To estimate the ligand association rates, spectral changes of the heme of *Ec* DOS were monitored after the addition of cyanide or imidazole. We assume that ligand-*Ec* DOS is generated via a pseudo-first-order reaction ($v = k_{obs}$[*Ec* DOS], $k_{obs} = k_{on}$[Ligand] + k_{off}) where [*Ec* DOS] is much lower than [Ligand]. As the actual time course for the change by cyanide in heme absorbance for the wild-type, Met95, Arg97, and Phe113 mutant proteins (except M95A and M95L mutants) exhibited monophasic kinetics, the observed rate constant (k_{obs}) was obtained by fitting to an exponential function, $A_{total} = A \exp(-k_{obs}t)$. In view of the biphasic kinetics of the M95A and M95L mutants, the observed rate constants were calculated by fitting to a double exponential function of $A_{total} = A_{fast} \exp(-k_{obs,fast}t) + A_{slow} \exp(-k_{obs,slow}t)$. The plots of k_{obs} versus [Ligand] exhibited a linear relationship (data not shown), leading to the calculation of k_{on} values for each phase from the equation $k_{obs} = k_{on}$[Ligand] + k_{off}. For imidazole binding, however, the actual time course for change in absorbance of heme for the wild-type and all mutant proteins exhibited monophasic kinetics. Thus, the observed rate constant (k_{obs}) was obtained by fitting to an exponential function of $A_{total} = A \exp(-k_{obs}t)$.

Cyanide dissociation experiments were performed by diluting the cyanide-bound heme protein (30−50 mM cyanide, 5−10 μM heme) solution into 1 mL of buffer. Prior to the reaction, excess cyanide was separated from CN-*Ec* DOS using a Sephadex G-25 desalting chromatography column (GE Healthcare, Amersham Pharmacia, Buckinghamshire, U.K.). Since cyanide dissociation reactions of the M95A, M95L, F113L, and F113T mutant proteins were not observed due to rapid association, 100 mM imidazole was added to the reaction buffer to prevent rebinding of cyanide. All dissociation reactions followed pseudo-first-order reaction

kinetics. Accordingly, dissociation rates were calculated by curve-fitting to a single exponential function.

Phosphodiesterase Assay. Wild-type and mutant proteins were diluted in PDE buffer (50 mM Tris-HCl at pH 8.0, 50 mM NaCl, and 5 mM $MgCl_2$). The cyanide and imidazole-bound wild-type and mutant enzymes, except F113Y, were prepared by adding 5 mM KCN or 50 mM imidazole, respectively. Because of the low affinity of the F113Y mutant protein for cyanide, the Fe(III)-CN-complex in this case was prepared in the presence of 10 mM KCN. However, the amount of Fe(III)-imidazole complex of F113Y formed under these conditions was insufficient to measure phosphodiesterase activity.

Colorimetric methods were used to determine phosphodiesterase activity, on the basis of earlier reports (*1*). Briefly, *Ec* DOS hydrolyzes c-diGMP to l-diGMP. CIAP catabolizes l-diGMP to GpG (guanylyl (3′,5′) guanosine) and phosphate. Phosphate was quantified colorimetrically using Biomol Green reagent (Biomol). The change in absorbance at 630 nm was measured with a Benchmark Microplate Reader (Bio-Rad Laboratories, Hercules, CA) and used to determine phosphate concentrations by comparison with a standard curve. Phosphodiesterase reaction conditions have been described previously (*1*).

RESULTS

In the present study, we examine the catalytic activity of the Fe(III) complex-bound full-length *Ec* DOS in the absence and presence of the external ligands, cyanide and imidazole. The major objective of this study is to establish the roles of Met95, Arg97, and Phe113 that are possibly located on the heme distal side, in catalysis and ligand binding kinetics. Note that the X-ray crystal structure of the heme distal side of *Ec* DOS-PAS was determined only for the Fe(II) complex, but the heme distal structure (in particular, between residues 86 and 97) for the Fe(III) complex was not determined because of its flexibility (*12*). Water or hydroxide appears to the axial ligand trans to His77, an internal axial ligand, for the Fe(III) complex. Prior to the measurement of catalysis, we analyzed the spectral characteristics of full-length wild-type and mutant *Ec* DOS in the absence and presence of cyanide and imidazole.

Optical Absorption Spectral Bands of Mutant Proteins without and with the External Ligands. Selective optical absorption spectra of the wild-type, M95A, F113L, and F113Y full-length *Ec* DOS are shown in Figure 1. All protein spectra with and without the external ligands are summarized in Table 1 and depicted in Figure 1S (Supporting Information). The wild-type protein has a low-spin Fe(III) complex. However, M95A, M95L, F113L, and F113T mutant proteins appear to partially contain the high-spin Fe(III) complex, in view of the small increase in absorption at around 638−641 nm (*7, 10*). Mutations in Met95, which is not coordinated to the Fe(III) complex, should result in displacement of the hydroxide or water ligand and lead to the establishment of a 5-coordinated high-spin complex. This is especially true for the M95A mutant, in which the space occupied by the side chain is smaller than that of the wild-type residue. It is presumed that a second sphere interaction is involved in displacement of the ligand by the mutations at Met95.

The Soret bands of these high-spin complexes are located between 412 and 415 nm, which are slightly shorter than

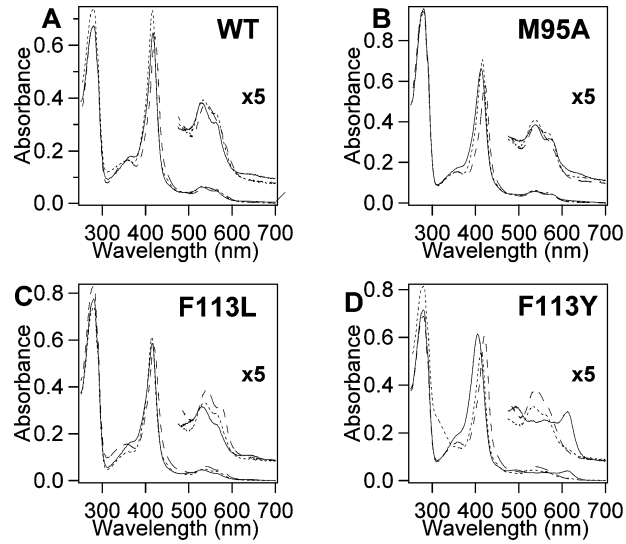

FIGURE 1: Selective optical absorption spectra of the full-length wild-type (5 μM) (A), M95A (5 μM) (B), F113L (5 μM) (C), and F113Y (5 μM) (D) mutant proteins. Spectra in the absence of ligands are shown as solid lines, whereas those with cyanide and imidazole are depicted by broken and dotted lines, respectively. Spectra of other full-length mutant enzymes without and with cyanide or imidazole are presented in Figure 1S (Supplementary Information). Buffer: 50 mM Tris-HCl and 50 mM NaCl at pH 8.0.

Table 1: Optical Absorption Spectral Maxima (nm) of the Fe(III) Complexes of Full-Length Wild-Type, Met95, Arg97, and Phe113 *Ec* DOS Proteins in the Absence and Presence of Cyanide and Imidazole[a]

	Fe(III)				Fe(III)-CN			Fe(III)-Imidazole		
Ec DOS	Soret	visible			Soret	β	α (shoulder)	Soret	β	α
WT	417	530	562		421	540	580	416	532	563
M95A	412	536	574	640	421	540	580	416	536	566
M95L	412	537	579	641	421	540	579	416	541	574
M95H	416	532	563		421	540	577	416	532	563
R97A	418	530	564		422	540	577	416	533	562
R97I	418	529	563		422	541	575	416	531	562
R97E	417	530	563		422	539	574	416	534	562
F113L	415	534	572	638	420	541	573	415	536	562
F113T	414	526	562	640	420	540	571	415	535	562
F113Y	405	494		613	421	538	572	413[b]	532[b]	561[b]

[a] All cyanide- and imidazole-bound forms are 6-coordinate low-spin. WT, wild type. [b] The F113Y mutant spectrum was obtained in the presence of 480 mM imidazole.

the wavelengths (416−417 nm) of the wild-type and other mutant proteins displaying the low-spin Fe(III) complex. Previous reports suggest that the His imidazole is directly bound to the Fe(III) complex in the M95H enzyme, although the Soret band (416 nm) is slightly shorter than that of wild-type protein (417 nm) (*10*). This hypothesis is confirmed by the finding that the binding rate constants of cyanide and imidazole to M95H are extremely low, compared with those of M95A, M95L, and wild-type protein (see Tables 3 and 4 in the later subsection). Moreover, the Soret and visible absorption bands of F113Y are located at 405 and 494 nm, respectively, which are shorter than those of other Fe(III) complex-bound proteins (412−418 nm and 526−537 nm). It is likely that in F113Y, the -O^- group of the Tyr residue directly coordinates to the Fe(III) complex.

In the CN-Fe(III) complex-bound *Ec* DOS spectrum, Soret bands are located around 420−422 nm and β-bands at around 538−541 nm, typical of a cyanide-bound low-spin 6-coor-

Table 2: Phosphodiesterase Activities (min^{-1}) of the Fe(III) Forms of Wild-Type, Met95, Arg97, and Phe113 Mutant *Ec* DOS Enzymes in the Absence or Presence of Cyanide and Imidazole[a]

Ec DOS	Fe(III)	Fe(III)-CN	Fe(III)-imidazole	fold activation
WT	8.1 (1.0)	86 (11)	85 (10)	10−11
H77A[b]	50 (6.2)			
M95A	15 (1.9)	71 (8.8)	55 (6.8)	3.7−4.7
M95L	19 (2.5)	75 (9.3)	76 (9.4)	3.9−4.0
M95H	11 (1.4)	86 (11)	55 (6.8)	5.0−7.8
R97A	8.0 (0.99)	34 (4.2)	51 (6.3)	4.3−6.4
R97I	13 (1.6)	73 (9.0)	97 (12)	5.6−7.5
R97E	11 (1.4)	27 (3.3)	72 (8.9)	2.5−6.5
F113L	14 (1.7)	84 (10)	88 (11)	6.0−6.3
F113T	7.0 (0.86)	84 (10)	101 (12)	12−14
F113Y	11 (1.4)	56 (6.9)	n.d.[c]	5.1

[a] Numbers in parentheses indicate the fold increase in activity, compared with that of the ligand-free full-length wild-type enzyme. Precise low-spin Fe(III) complex formation of the enzyme upon the addition of external ligand was confirmed by monitoring the optical absorption spectra of the heme-complexed enzyme before initiation of the catalytic reaction. WT, wild type. [b] The H77A mutant has very low heme binding ability. Catalytic activity of the H77A mutant *Ec* DOS was measured in the presence of 10 mM DTT. [c] Phosphodiesterase activity of the F113Y *Ec* DOS with Fe(III)-imidazole could not be measured due to low affinity for imidazole.

Table 3: Kinetic Parameters of the Binding of Cyanide to the Fe(III) Complexes of Full-Length Wild-Type, Met95, Arg97, and Phe113 Mutant *Ec* DOS Proteins[a]

	k_{on} ($\times 10^{-5}$ $\mu M^{-1}min^{-1}$)	k_{off} ($\times 10^{-3}$ min^{-1})	K_d (μM)[b]
WT	30 ± 9.0	n.d.	
M95A fast	19,000 ± 1,100	2.3 ± 2.1	0.012
slow	3,400 ± 540		
M95L fast	19,000 ± 2,300	1.9 ± 0.1	0.010
slow	4,500 ± 420		
M95H	4.9 ± 0.18	n.d.	
R97A	7.0 ± 1.2	5.8 ± 2.3	83
R97I	8.3 ± 0.2	5.5 ± 0.6	66
R97E	2.1 ± 1.3	6.9 ± 1.4	330
F113L	5,300 ± 78	1.3 ± 0.1	0.025
F113T	150 ± 19	2.1 ± 2	1.4
F113Y	0.091 ± 0.006	14 ± 6	15,000

[a] Data are presented as average values of at least three experiments. WT, wild type. [b] K_d values (equilibrium dissociation constants) were calculated as the k_{off} divided by the k_{on} value.

Table 4: Kinetic Parameters of the Binding of Imidazole to Fe(III) Complexes of Full-Length Wild-Type, Met95, Arg97, and Phe113 Mutant *Ec* DOS Proteins[a]

	k_{on} ($mM^{-1}s^{-1}$)	k_{off} (s^{-1})[b]	K_d (mM)
WT	0.32 ± 0.008	0.77	2.4 ± 0.4
M95A	3.7 ± 0.1 × 10^3	23	0.0061 ± 0.0006
M95L	0.53 ± 0.2 × 10^3	5.8	0.011 ± 0.001
M95H	n.d. [c]		
R97A	0.55 ± 0.03	1.7	3.0 ± 0.3
R97I	1.5 ± 0.09	0.65	0.43 ± 0.1
R97E	0.25 ± 0.02	0.98	3.9 ± 0.9
F113L	44 ± 4	5.7	0.13 ± 0.02
F113T	1.6 ± 0.3	4.0	2.5 ± 1.1
F113Y	0.064 ± 0.014	6.0	93 ± 8.3

[a] Data are presented as average values obtained from at least three experiments. WT, wild type. [b] k_{off} values (dissociation rate constants) were obtained by multiplying K_d by the k_{on} values. [c] Spectral changes of the M95H mutant in the presence of imidazole were too small to determine the association rate constant for imidazole to the Fe(III) enzyme.

dinate Fe(III) complex (*11, 14*). No marked differences were evident between the wild-type and mutant cyanide-bound Fe(III) proteins, although the α-bands at the shoulder are

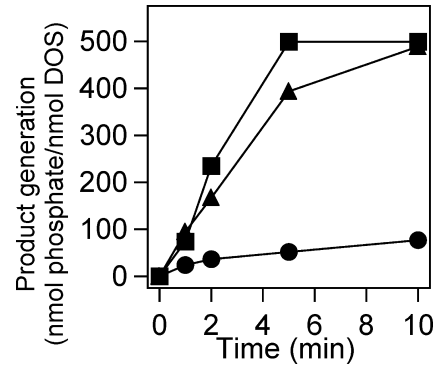

FIGURE 2: Time-course of l-diGMP hydrolysis by Fe(III) (●), Fe(III)-cyanide (■), and Fe(III)-imidazole (▲) complexes of the full-length wild-type enzyme.

scattered between 571 and 580 nm. For imidazole-Fe(III) complex-bound *Ec* DOS, Soret bands were present at around 413−416 nm, whereas the β- and α-bands were located around 532−541 nm and 562−574 nm, respectively. These bands are typical of the bis-imidazole-bound low-spin 6-coordinate Fe(III) complex (*10*).

Phosphodiesterase Activities of Ec DOS Enzymes. The phosphodiesterase activity of the Fe(III) complex-bound enzyme (8.1 min^{-1}) was comparable to that of the Fe(II) complex-bound enzyme (9.7 min^{-1}) (*1*). The binding of cyanide or imidazole to Fe(III) complex-bound *Ec* DOS substantially enhanced activity by 10- to 11-fold (up to 86 min^{-1}) (Table 2, Figure 2). This fold increase observed for Fe(III) complex-bound *Ec* DOS by adding the external axial ligands was higher than that reported for the Fe(II) complex-bound enzyme in the presence of O_2, CO, or NO gas (6.3- to 7.2-fold) (*1*).

Next, we examined whether binding of the heme iron complex to the sensor domain of *Ec* DOS is essential for phosphodiesterase activity. His77 is the axial ligand for the heme iron in the sensor domain of *Ec* DOS, and thus, the H77A mutant has very low heme binding ability (*9, 15*). The phosphodiesterase activity of the H77A mutant protein was 50 min^{-1}. This value is relatively high, i.e., more than half-that of the ligand-induced wild-type enzyme (Table 2). Therefore, we conclude that binding of the heme iron complex to the *Ec* DOS sensor domain is not essential for catalysis and that the heme iron suppresses catalysis of the enzyme.

The basal activities of M95A and M95L mutant proteins (15−19 min^{-1}) were 2-fold higher than that of the wild-type enzyme (8.1 min^{-1}), whereas activities of M95H, R97A, R97I, and R97E proteins (8−13 min^{-1}) were only slightly higher than those of the wild-type, M95A, and M95L mutant proteins. The basal catalytic activities of F113L, F113T, and F113Y enzymes (7−14 min^{-1}) were also similar or slightly higher than that of the wild-type enzyme.

The catalytic activities of Met95, Arg97, and Phe113 mutant enzymes were enhanced by adding cyanide and imidazole, similar to that of the wild-type protein (Table 2, Figure 3). However, the fold activation of the mutant proteins (2.5- to 7.8-fold) induced by adding external ligands (except F113T) (12- to 14-fold) was lower than those (10- to 11-fold) observed for the wild-type enzyme (Table 2). Cyanide-induced enhancement of the M95A and M95H mutant enzymes was more marked than that by imidazole, whereas

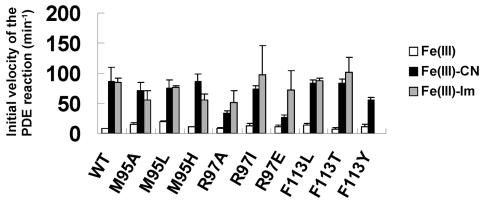

FIGURE 3: Comparison of the catalytic activities of the Fe(III) (white), Fe(III)-cyanide (black), and Fe(III)-imidazole (gray) complexes of the full-length wild-type, Met95, Arg97, and Phe113 mutant *Ec* DOS proteins.

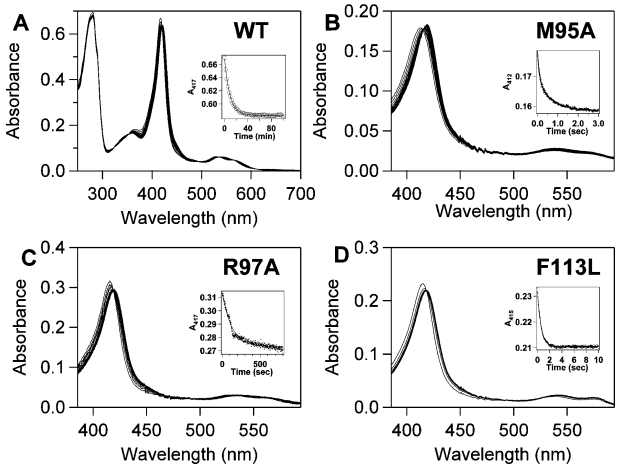

FIGURE 4: Soret absorption spectral changes accompanying the binding of cyanide to the full-length wild-type (5 μM) (left in A), M95A (2.5 μM) (left in B), R97A (2.5 μM) (left in C), and F113L (2.5 μM) (left in D) mutant *Ec* DOS proteins. The insert in the each figure shows time-dependent spectral changes monitored at the indicated wavelengths. Buffer: 50 mM Tris-HCl and 50 mM NaCl at pH 8.0.

imidazole-induced enhancement of Arg97 mutants was more pronounced than that by cyanide (Figure 3). This opposite effect of ligands may reflect differences in ionic and/or van der Waals interactions between the side-chains of the mutated amino acids and ligands.

Kinetic Parameters of Cyanide Binding to the Fe(III) Complex of Mutant Proteins. To clarify the ligand access channel or distal side structure of the Fe(III) complex, we examined the binding and dissociation kinetics of cyanide for wild-type and full-length mutant *Ec* DOS enzymes (summarized in Table 3). Cyanide binding is biphasic for the M95A and M95L proteins, and monophasic for the wild-type and other mutant proteins (Table 3; selected results are shown in Figure 4). The binding rate constants (19,000 $\times$ 10^{-5} $\mu M^{-1}min^{-1}$) of cyanide to the Fe(III) complex-bound M95A and M95L enzymes were 633-fold higher than that to the wild-type enzyme (30 $\times$ 10^{-5} $\mu M^{-1}min^{-1}$). Even for the slow phase, rate constants to these mutant proteins were >100-fold higher, compared to that of the wild-type enzyme. Interestingly, the binding rate constant to M95H was significantly lower than those to M95A and M95L, and 6-fold lower than that of the wild-type. The results clearly indicate that Met95 is located at the ligand access channel and that the imidazole group of His95 in M95H appears directly bound to the heme iron as the sixth axial ligand and hampers ligand binding. However, the hydroxide anion (or water) ligand in the heme-distal side is seen in the crystal structure, although the loop containing Met95 is disordered in the Fe(III) complex-bound sensor domain (*12*). The rate constant

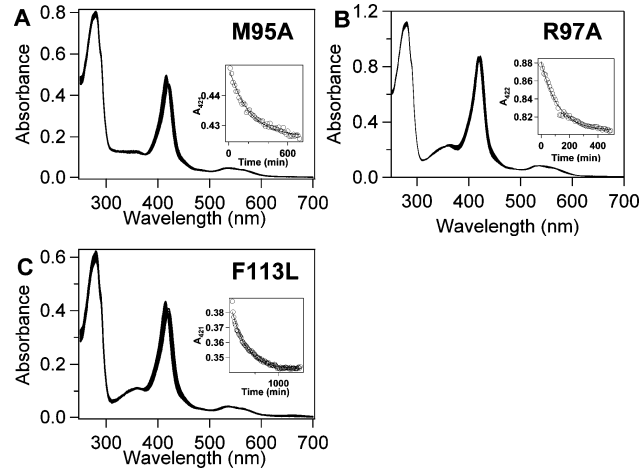

FIGURE 5: Soret absorption spectral changes accompanying the dissociation of cyanide from the full-length M95A (left in A), R97A (left in B), and F113L (left in C) mutant *Ec* DOS proteins. The insert in each figure shows time-dependent spectral changes monitored at the indicated wavelengths. Buffer: 50 mM Tris-HCl and 50 mM NaCl at pH 8.0.

for cyanide binding to F113L was >3-fold lower than that for the Met95 mutant. However, the constant (5,300 $\times$ 10^{-5} $\mu M^{-1}min^{-1}$) for cyanide binding to the Fe(III) complex of the F113 protein was 176-fold higher than that of the wild-type protein. Mutant proteins with high rate constants display a 5-coordinated high-spin Fe(III) complex (Table 1) where the sixth axial coordination position is vacant, and the fifth internal axial ligand should be His imidazole. This coordination structure of mutant proteins is distinct from that of the wild-type protein, which displays a 6-coordinate low-spin Fe(III) complex where the sixth position is occupied by hydroxide or water (*12*).

The rate constants (2.1−8.3 $\times$ 10^{-5} $\mu M^{-1}min^{-1}$) for cyanide binding to other mutant proteins, M95H, R97A, R97I, and R97E, were several-fold lower than that to the wild-type enzyme, suggesting the existence of ionic and/or van der Waals repulsion forces for binding to the heme complex in mutant enzymes. Interestingly, the rate constant for cyanide binding to F113Y (0.0 91 $\times$ 10^{-5} $\mu M^{-1}min^{-1}$) was 330-fold lower than that of the wild-type protein. As suggested earlier, direct coordination of the phenoxylate oxygen of Tyr with the heme iron may restrict interactions with the external ligand, cyanide.

It was not possible to evaluate the dissociation rate constant for cyanide from the wild-type full-length *Ec* DOS because of protein instability (*14*). The dissociation rate constants for cyanide from mutant proteins were between 1.9 and 6.9 $\times$ 10^{-3} min^{-1}, whereas that for F113Y was 14 $\times$ 10^{-3} min^{-1}. As a result, the apparent equilibrium dissociation constant (15,000 μM) of F113Y was significantly higher than those of other mutant proteins (0.025−330 μM). The results consistently support the hypothesis that binding of the phenoxylate oxygen of the Tyr113 residue in F113Y hinders binding of the external ligand, cyanide, to the Fe(III) complex.

Kinetic Parameters of Imidazole Binding to the Fe(III) Complex of Mutant Proteins. Imidazole binding rate constants were evaluated using a stopped-flow spectrometer (Table 4, Figures 6 and 7). The rate constants (0.53−3.7 $\times$ 10^{3} $mM^{-1}s^{-1}$) for imidazole binding to M95A and M95L

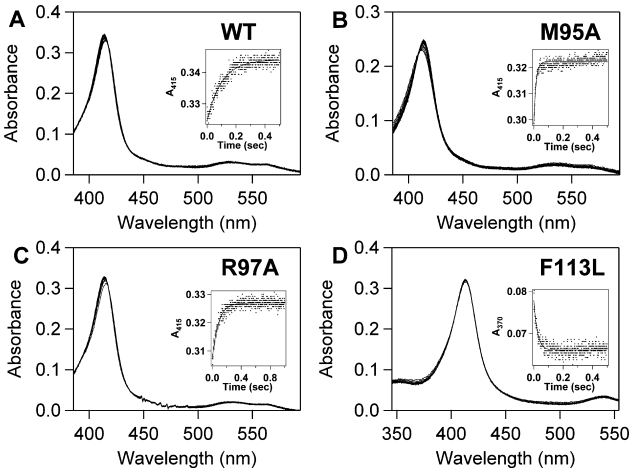

FIGURE 6: Soret absorption spectral changes accompanying the binding of imidazole to full-length wild-type (2.5 μM) (left in A), M95A (2.5 μM) (left in B), R97A (2.5 μM) (left in C), and F113L (2.5 μM) (left in D) mutant *Ec* DOS proteins. The insert in each figure shows time-dependent spectral changes monitored at the indicated wavelengths. Buffer: 50 mM Tris-HCl and 50 mM NaCl at pH 8.0.

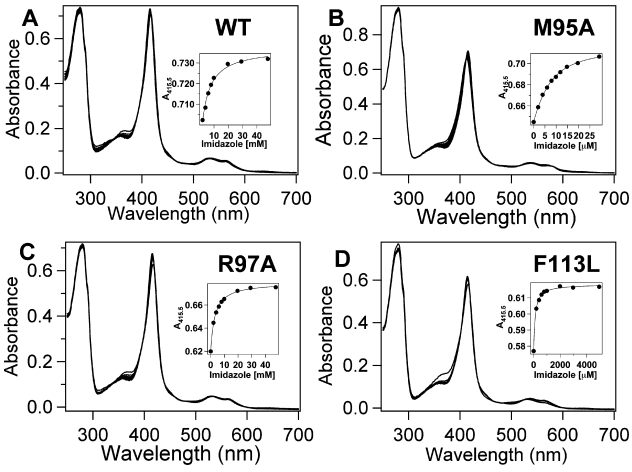

FIGURE 7: Soret absorption spectral changes accompanying the titration of imidazole into a solution containing the full-length wild-type (5 μM)(left in A), M95A (5 μM) (left in B), R97A (5 μM) (left in C), and F113L (5 μM) (left in D) mutant *Ec* DOS proteins. The insert in each figure shows time-dependent spectral changes monitored at the indicated wavelengths. Buffer: 50 mM Tris-HCl and 50 mM NaCl at pH 8.0.

were more than 3 orders of magnitude higher than that (0.32 $mM^{-1}s^{-1}$) of binding to the wild-type protein (Table 4). However, it was not feasible to observe distinct binding of imidazole to the heme iron of M95H in terms of absorption spectroscopy. The rate constant (44 $mM^{-1}s^{-1}$) for imidazole binding to F113L was 138-fold higher than that of the wild-type protein, while that of F113Y (0.064 $mM^{-1}s^{-1}$) was lower. These trends were similar to those observed for cyanide binding. Our findings strongly indicate that Met95 and Phe113 are located at the ligand access channel in the heme distal side of the Fe(III) complex-bound sensor domain. This hypothesis is corroborated by the finding that direct coordination of imidazole to the Fe(III) complex of M95H and the phenoxylate oxygen of Tyr113 in F113Y forms a 6-coordinated low-spin complex and hampers binding of the external imidazole molecule to the heme iron. The dissociation rate constants for imidazole from wild-type and mutant proteins were not significantly different (Table 4). As a result, the equilibrium dissociation constants evaluated from the binding and dissociation rate constants (0.011−0.0061 mM) of the Met95 mutants were considerably lower than that of the wild-type protein (2.4 mM) (Table 4). Consistently, the equilibrium dissociation constant (93 mM) of F113Y was 39-fold higher than that of the wild-type protein, reinforcing the concept that direct coordination of the -O^- group of Tyr to the Fe(III) complex restricts imidazole binding.

DISCUSSION

In a previous study, we demonstrated that *Ec* DOS is the gas-responsive heme-sensor enzyme. Binding of gas molecules, such as O_2, CO, or NO, to the Fe(II) heme-bound form of the enzyme markedly enhances phosphodiesterase activity toward c-diGMP, leading to the generation of l-diGMP (*1*). All other gas-responsive heme-sensor proteins reported hitherto recognize and respond to selective gas molecules; for instance, FixL displays specificity for O_2, CooA for CO, CBS for CO, and sGC for NO (*2*−*5, 16, 17*). Therefore, the behavior of *Ec* DOS is unprecedented and novel in that the enzyme does not discriminate among O_2, CO, and NO. In addition, the redox potential of *Ec* DOS is not as high as those of cytochromes *c* and b_{562}, and most complex-bound species purified by the overexpression system under our experimental conditions contain Fe(III) (see Introduction). This may be because of artifacts caused by limiting amounts of the redox partner and/or the isolation procedure. It is necessary to establish how the Fe(III) complex-bound form of *Ec* DOS responds to the interacting ligand. Here, we show that binding of external ligands, such as cyanide and imidazole, to the Fe(III) complex-bound enzyme substantially enhances phosphodiesterase activity toward c-diGMP. Importantly, the heme-free mutant enzyme displays comparable catalytic activity to ligand-stimulated enzymes, suggesting that the heme is not essential for catalysis but that its binding to the sensor domain is important to suppress catalysis. Moreover, mutation of the putative distal amino acids, Met95, Arg97, and Phe113, significantly influenced catalysis by the Fe(III) complex-bound enzyme and substantially altered the binding kinetics or equilibrium dissociation constants for external ligands.

Cyanide Binding. Previous reports have described significant differences in the kinetic parameters of cyanide binding to wild-type and Met95 mutant proteins (*11, 14, 20*). Experimental conditions differ in two respects between previously reported work and the present article. First, we used full-length proteins, whereas earlier papers principally employed isolated PAS domains. Second, the pH values at which kinetic data were obtained differ between previous papers and the present work. The k_{on} values, at pH 7.5, for binding of cyanide to the isolated wild-type PAS domain were 2.7×10^{-3} $\mu M^{-1}min^{-1}$ (*11, 14*) and 2.5×10^{-3} $\mu M^{-1}min^{-1}$ (*20*). There values are very similar. For the full-length wild-type enzyme, however, the k_{on} value at pH 7.5 was reported to be 13×10^{-5} $\mu M^{-1}min^{-1}$ (*14*), whereas the k_{on} value at pH 8.0 was 30×10^{-5} $\mu M^{-1}min^{-1}$ in the present study (Table 3). Differences in kinetic parameters shown by the isolated heme-bound PAS domain and the full-length enzyme would arise because of global structural differences between the two proteins; it is possible that the C-terminal domain covers the ligand access channel for the heme

domain, as has been suggested previously (*7, 14*). The k_{on} value for the full-length enzyme in the present article is 2.3-fold higher than that reported previously. The only difference in experimental conditions is that the present data on catalytic and kinetic parameters were obtained at pH 8.0, whereas earlier figures were measured at pH 7.5. The kinetics of cyanide binding to the heme pocket of myoglobin (axial ligands water or OH^-, and His) is regulated by several critical factors (*20, 22, 23*). These include the ease of water displacement from the ferric ion, the acid dissociation constant of HCN inside the heme pocket, and steric hindrance and electrostatic interactions at the sixth coordination position. Involvements of ionic characters for binding of other ligands such as fluoride or azide to myoglobin and FixL were reported (*24*−*26*). Therefore, small pH differences may significantly affect cyanide binding affinity to a heme protein. In fact, the recent excellent paper on pH dependence for cyanide binding to the Fe(III) complex of the isolated PAS domain of *Ec* DOS has revealed that this is likely (*23*). It is probable that experimental pH differences significantly affect measured k_{on} values for the full-length enzyme.

Furthermore, the k_{on} values for cyanide binding to the isolated PAS domain of the M95A and M95L mutants have been previously reported to be 11- and 8-fold higher, respectively, than that to the wild-type protein (*14*). The k_{on} values for full-length enzymes with the same Met95 mutations were 633-fold higher than that to the wild-type protein (Table 3). Similarly, the full-length M95H mutant showed a 6-fold lower k_{on} value than did the wild- type protein (Table 3), whereas the isolated PAS domain of the same mutant exhibited a k_{on} value 17-fold lower than wild-type (*14*). We again attribute these differences to structural variations in the heme environment of the isolated PAS domain compared to the full-length protein. Notably, the isolated heme-bound PAS domain is a dimer, whereas the full-length protein forms a tetramer (*8, 15*).

Physiological Significance of the Fe(III) Complex-bound Enzyme. Redox equilibrium should exist between the Fe(II) complex-bound and Fe(III) complex-bound *Ec* DOS forms within cells, depending not only on environmental stimuli but also on the nature of the proximal partner supplying reducing equivalents. The O_2 sensor enzymes, FixL and AxPDEA1, and the NO sensor enzyme, sGC, function in response to their respective gas molecules in the Fe(II) complex state. The autoxidation rate is very low for AxPDEA1. Additionally, for sGC, O_2 does not even bind to the Fe(II) complex. As a result, these proteins appear to take up the stable Fe(II) complex form within cells and function as gas-sensor enzymes using redox characteristics with bias in favor of the Fe(II) complex. However, the O_2 molecule binds easily to the Fe(II) complex of *Ec* DOS with a rapid autoxidation rate, compared with those of other gas sensor enzymes. Moreover, the redox potential of the isolated heme-bound domain of *Ec* DOS is relatively high (+70 mV vs SHE) (*9, 10*), further supporting the hypothesis that the redox state is biased to favor the Fe(III) complex over the Fe(II) complex under specific conditions. Again, equilibrium between the Fe(III) and Fe(II) species in cells is biased toward the Fe(III) form under various oxidative or nitrosative conditions. Therefore, it is reasonable to assume that the *Ec* DOS enzyme in the Fe(III) complex form exists in response to external stimuli under oxidative stress conditions. While the heme-free *Ec* DOS enzyme displays sufficient catalytic activity, it is unlikely that heme association or dissociation regulates its function as a heme-responsive sensor enzyme. Very tight heme binding to the *Ec* DOS apo-protein further refutes the hypothesis that *Ec* DOS is the heme-responsive heme-sensor protein (*15*).

Phosphodiesterase activities of the isolated functional domain of *Ec* DOS in the absence of the sensor domain under different experimental conditions have been reported (*19*). Data from the present study show that the full-length enzyme devoid of the heme iron has comparable catalytic activity to ligand-stimulated enzymes under similar experimental conditions. We propose that the heme iron complex bound to the sensor domain acts in catalytic suppression, which is released by binding of an external axial ligand.

Physiological Significance of External Ligands for the Fe(III) Complex-Bound Enzyme. The types of ligand that bind to the Fe(III) complex of *Ec* DOS under physiological conditions are yet to be identified. We propose that the *Ec* DOS enzyme is ready to receive any external axial ligand at both heme redox states and that catalytic regulation is conducted in response to external stimuli via ligand binding to both the Fe(II) and Fe(III) complexes. Alternatively, perhaps more importantly, equilibrium between the Fe(III) and Fe(II) species in response to oxidative (H_2O_2 or superoxide induced) or nitrosative stress is probably critical for the catalytic regulation of *Ec* DOS in case no distinct external axial ligand for the Fe(III) complex in the cells exists. One possibility is that the Fe(III) form is inactive, while the Fe(II) form is resting and the Fe(II)-O_2 form is active, and thus, *Ec* DOS is the oxygen sensor enzyme. Further studies are required to confirm this hypothesis.

Significance of the Putative Distal Amino Acids in Catalysis. The X-ray crystal structure of the isolated heme-bound sensor domain of *Ec* DOS indicates that Met95 is the axial ligand for the Fe(II) complex, Arg97 is the direct binding site for O_2, and Phe113 is located in the vicinity of the O_2 bound to the Fe(II) complex (*12, 13*). In a previous study by our group, mutations at Met95, but not Arg97, significantly influenced the regulation of the catalytic activity of Fe(II) complex-bound *Ec* DOS (*1*). X-ray crystal analyses additionally support profound structural alterations, including axial ligand switch, upon heme redox changes of the heme iron complex of *Ec* DOS (*12*). However, the heme distal structure of the Fe(III) complex-bound form could not be determined because of its considerable flexibility. It is important to establish the roles of the amino acids located at the heme distal side of the Fe(III) complex-bound enzyme and the ligand access channel in catalysis. Therefore, Met95, Arg97, and Phe113 of the Fe(III) complex-bound enzyme were subjected to site-directed mutagenesis with a view to clarifying their roles in catalysis and ligand binding kinetics.

Mutations at these residues significantly increased the basal activity and suppressed ligand-stimulated catalytic activity in that fold activation (3.7- to 7.8-fold) induced by ligands for mutant proteins was less than that for the wild-type protein (10- to 11-fold), except in the case of F113T (Table 2). Increases in the basal activities of the Met95 mutant proteins were similar to those observed for the Fe(II) complex-bound enzyme (*1*). Moreover, ligand-dependent catalytic enhancement was distinct between the Met95 and Arg97 mutant proteins. Catalytic enhancement of R97I by

imidazole was more marked than that of wild-type and Met95 mutant *Ec* DOS proteins (Figure 3). We assume that the relatively large and hydrophobic molecules of imidazole interact with residue 97, which is at the optimal position or orientation for interactions, relative to position 95. Our findings collectively suggest that Met95, Arg97, and Phe113 are located at the heme distal side, and thus influence basal catalytic activities and ligand-induced catalytic enhancement.

Significance of the Putative Distal Amino Acids in Ligand Binding. Optical absorption spectra of the Met95 and Phe113 mutant proteins indicate that the 5-coordinated high-spin structure is generated by the mutations (Table 1). On the basis of the results, we assume that these residues are located in close proximity to the Fe(III) complex bound to the enzyme. Binding rate constants for both cyanide and imidazole to the Met95 mutant proteins were substantially higher than those to wild-type protein, further confirming that Met95 is positioned close to the ligand access channel or at the heme distal side. In this regard, Phe113 appears more influential for ligand binding than Arg97. Accordingly, we hypothesize that Arg97 is more distant from the heme iron than Phe113 in the Fe(III) complex-bound protein.

In our previous experiments on cyanide binding to the Fe(III) complex-bound isolated PAS domain of *Ec* DOS, M95A and M95L mutations enhanced the binding rate from 0.045 $mM^{-1}s^{-1}$ (wild-type) to 0.50 (M95A) or 0.38 (M95L) $mM^{-1}s^{-1}$ (*14*). More substantial effects of the Met95 substitutions were observed in the present study using full-length proteins. In fact, the rate constant for cyanide binding to the isolated wild-type PAS domain was 20-fold higher than that of the full-length enzyme, further suggesting that the ligand access channels of the two proteins are distinct (*14*). Therefore, despite the failure to resolve the position of Met95 by crystal structure analysis (*12*), we presume that the residue is located close to the ligand access channel, substantially influencing enzyme kinetics.

Our data collectively indicate that these amino acids are located in the heme distal side of the Fe(III) complex-bound *Ec* DOS and affect catalysis and ligand binding kinetics. These amino acids do not directly interact or coordinate to the Fe(III) complex. The second phase interactions on the heme distal side may be involved in the results, which are similar to those observed for the mutants at Leu99 and Leu115 in the second hydrophobic contact (*27*).

Summary. The major findings of the present study are as follows: (i) Fe(III) complex-bound *Ec* DOS displays sufficient catalytic activity toward c-diGMP comparable to that of the Fe(II) complex-bound enzyme, (ii) cyanide and imidazole binding to the Fe(III) complex-bound enzyme substantially enhance catalytic activity, (iii) the heme-free enzyme displays comparable catalytic activity to the ligand-stimulated enzyme, and (iv) mutations at Met95, Arg97, and Phe113 significantly influence catalysis, absorption spectra, and ligand binding kinetics. On the basis of these findings, we propose that (i) the heme of *Ec* DOS functions to suppress catalysis, (ii) binding of external ligands to the heme iron releases catalytic suppression, irrespective of the heme redox state, and (iii) Met95, Arg97, and Phe113 are located at the heme distal side of the Fe(III) complex-bound enzyme in sufficiently close proximity to significantly influence catalysis, absorption spectra and ligand binding kinetics. Note that Arg97 and Phe113 play critical roles in the recognition of O_2 and stability of the O_2 complex of the Fe(II) form at the initial stage of intramolecular signal transduction of catalysis of *Ec* DOS (*20, 21*).

SUPPORTING INFORMATION AVAILABLE

Optical absorption spectra of the ligand-free, cyanide-bound, and imidazole-bound Fe(III) hemin-bound full-length wild-type, M95A, M95L, M95H, R97A, R97I, R97E, F113L, F113T, and F113Y *Ec* DOS proteins. This material is available free of charge via the Internet at http://pubs.acs.org.

REFERENCES

1. Tanaka, A., Takahashi, H., and Shimizu, T. (2007) Critical role of the heme axial ligand, Met95, in locking catalysis of the phosphodiesterase from *Escherichia coli* (*Ec* DOS) toward Cyclic diGMP. *J. Biol. Chem. 282*, 21301–21307.
2. Sasakura, Y., Yoshimura-Suzuki, T., Kurokawa, H., and Shimizu, T. (2006) Structure-function relationships of *Ec* DOS, a heme-regulated phosphodiesterase from *Escherichia coli*. *Acc. Chem. Res. 39*, 37–43.
3. Gilles-Gonzalez, M. A., and Gonzalez, G. (2005) Heme-based sensors: defining characteristics, recent developments, and regulatory hypothesis. *J. Inorg. Biochem. 99*, 1–22.
4. Uchida, T., and Kitagawa, T. (2005) Mechanism for transduction of the ligand-binding signal in heme-based gas sensory proteins revealed by resonance Raman spectroscopy. *Acc. Chem. Res. 38*, 662–670.
5. Aono, S. (2003) Biochemical and biophysical properties of the CO-sensing transcriptional activator CooA. *Acc. Chem. Res. 36*, 825–831.
6. Gilles-Gonzalez, M. A., and Gonzalez, G. (2004) Signal transduction by heme-containing PAS-domain proteins. *J. Appl. Physiol. 96*, 774–783.
7. Taguchi, S., Matsui, T., Igarashi, J., Sasakura, Y., Araki, Y., Ito, O., Sugiyama, S., Sagami, I., and Shimizu, T. (2004) Binding of oxygen and carbon monoxide to a heme-regulated phosphodiesterase from *Escherichia coli*: Kinetics and infrared spectra of the full-length wild-type enzyme, isolated PAS domain, and Met95 mutants. *J. Biol. Chem. 279*, 3340–3347.
8. Sasakura, Y., Hirata, S., Sugiyama, S., Suzuki, S., Taguchi, S., Watanabe, M., Matsui, T., Sagami, I., and Shimizu, T. (2002) Characterization of a direct oxygen sensor heme protein from *Escherichia coli*: Kinetics of the heme redox states and mutations at the heme-biniding site on catalysis and structure. *J. Biol. Chem. 277*, 23821–23827.
9. Chang, A. L., Tuckerman, J. R., Gonzalez, G., Mayer, R., Weinhouse, H., Volman, G., Amikam, D., Benziman, M., and Gilles-Gonzales, M. A. (2001) Phosphodiesterase A1, a regulator of cellulose synthesis in *Acetobacter xylinum* is a heme-based sensor. *Biochemistry 40*, 3420–3426.
10. Hirata, S., Matsui, T., Sasakura, Y., Sugiyama, S., Yoshimura, T., Sagami, I., and Shimizu, T. (2003) Characterization of Met95 Mutants of a heme-regulated phosphodiesterase from *Escherichia coli*: Optical absorption, magnetic circular dichroism, circular dichroism, and redox potentials. *Eur. J. Biochem. 270*, 4771–4779.
11. Watanabe, M., Kurokawa, H., Yoshimura-Suzuki, T., Sagami, I., and Shimizu, T. (2004) Critical rols of Asp40 at the haem proximal side of haem-regulated phosphodiesterase from *Escherichia coli* in redox potential, auto-oxidation and catalytic control. *Eur. J. Biochem. 271*, 3937–3942.
12. Kurokawa, H., Lee, D. S., Watanabe, M., Sagami, I., Mikami, B., Raman, C. S., and Shimizu, T. (2004) A redox-controlled molecular switch revealed by the crystal structure of a bacterial heme PAS sensor. *J. Biol. Chem. 279*, 20186–20193.
13. Park, H., Suquet, C., Satterlee, J. D., and Kang, C. (2004) Insights into signal transduction Involving PAS domain oxygen-sensing heme proteins from the X-ray crystal structure of *Escherichia coli* DOS heme domain (*Ec* DOSH). *Biochemistry 43*, 2738–2746.
14. Watanabe, M., Matsui, T., Sasakura, Y., Sagami, I., and Shimizu, T. (2002) Unusual cyanide bindings to a heme-regualted phoephodiesterase from *Escherichia coli*: effect of Met95 mutations. *Biochem. Biophys. Res. Commun. 299*, 169–172.
15. Yoshimura, T., Sagami, I., Sasakura, Y., and Shimizu, T. (2003) Relationships between heme incorporation, tetramer formation, and catalysis of a heme-regulated phosphodiesterase from *Escherichia*

coli: A study of deletion and site-directed mutants. *J. Biol. Chem. 278*, 53105–53111.
16. Akimoto, S., Tanaka, A., Nakamura, K., Shiro, Y., and Nakamura, H. (2003) O_2-specific regulation of the ferrous heme-based sensor kinase FixL from *Sinorhizobium meliloti* and its aberrant inactivation in the ferric form. *Biochem. Biophys. Res. Commun. 304*, 136–142.
17. Tanaka, A., Nakamura, H., Shiro, Y., and Fujii, H. (2006) Role of the heme distal residues of FixL in O_2 sensing; A single convergent structure of the heme moiety is relevant to the dowunregulation of kinase activity. *Biochemistry 45*, 2515–2523.
18. Igarashi, J., Sato, A., Kitagawa, T., Yoshimura, T., Yamauchi, S., Sagami, I., and Shimizu, T. (2004) Activation of heme-regulated eukaryotic initiation factor 2α kinase by nitric oxide is induced by the formation of a five-coordinated NO-heme complex: Optical absorption, electron spin resonance, and resonance Raman spectral studies. *J. Biol. Chem. 279*, 15752–15762.
19. Schmidt, A. J., Ryjenkov, D. A., and Gomelsky, M. (2005) The ubiquitous protein domain EAL is a cyclic diguanylate-specific phosphodiesterase: Enzymatically active and inactive EAL domains. *J. Bacteriol. 187*, 4774–4781.
20. Ishitsuka, Y., Araki, Y., Tanaka, A., Igarashi, J., Ito, O., and Shimizu, T. (2008) Arg97 at the heme distal side of the isolated heme-bound PAS domain of a heme-based oxygen sensor from *Escherichia coli* (*Ec* DOS) plays critical roles in auto-oxidation and binding to gases, particularly O_2. *Biochemistry 47*, 9016–9028.
21. El-Mashtoly, S. F., Nakashima, S., Tanaka, A., Shimizu, T., and Kitagawa, T. (2008) Roles of Arg97 and Phe113 in regulation of distal ligand binding to heme in the sensor Domain of *Ec* DOS protein: Resonance Raman and mutation study. *J. Biol. Chem. 283*, 19000–19010.
22. Dou, Y., Olson, J. S., Wilkinson, A. J., and Ikeda-Saito, M. (1996) Mechanism of hydrogen cyanide binding to myoglobin. *Biochemistry 35*, 7107–7113.
23. Bidwai, A. K., Ok, E. Y., and Erman, J. E. (2008) pH Dependence of cyanide binding to the ferric heme domain of the direct oxygen sensor from *Escherichia coli* and the effect of alkaline denaturation. *Biochemistry 47*, 10458–10470.
24. Merryweather, J., Summers, F., Vitello, L. B., and Erman, J. E. (1998) Metmyoglobin/fluoride: Effect of distal histidine protonation on the association and dissociation rate constants. *Arch. Biochem. Biophys. 358*, 359–368.
25. Lin, J., Merryweather, J., Vitello, L. B., and Erman, J. E. (1999) Metmyoglobin/azide: The effect of heme-linked ionization on the rate of complex formation. *Arch. Biochem. Biophys. 362*, 148–158.
26. Winkler, W. C., Gonzalez, G., Wittenberg, J. B., Hille, R., Dakappagari, N., Jacob, A., Gonzalez, L. A., and Gilles-Gonzalez, M. A. (1996) Nonsteric factors dominate binding of nitric oxide, azide, imidazole, cyanide, and fluoride to rhizobial heme-based oxygen sensor FixL. *Chem. Biol. 3*, 841–850.
27. Yokota, N., Araki, Y., Kurokawa, H., Ito, O., Igarashi, J., and Shimizu, T. (2006) Critical roles of Leu99 and Leu115 at the heme distal side in auto-oxidation and the redox potential of a heme-regulated phosphodiesterase from *Escherichia coli*. *FEBS J. 273*, 1210–1223.

BI8012017